Binding energy of light nuclei using the noncritical holography model

M. R. Pahlavani* and R. Morad†

Department of Nuclear Physics, Faculty of Basic Science, University of Mazandaran, P.O. Box 47416-1467, Babolsar, Iran

(Received 10 July 2013; revised manuscript received 8 October 2013; published 26 December 2013)

The potential of light nuclei, such as deuteron, tritium, and helium isotopes, are studied using a noncritical holographic QCD model constructed in the six-dimensional anti–de Sitter (AdS_6) supergravity background. The nucleus potentials are considered as a sum of the nucleon-nucleon potentials. The nucleon-meson coupling constants evaluated from the noncritical holography QCD model are used to obtain these potentials. The potential of both ground state and available excited states of these nuclei are well studied using this model. The binding energy of nuclei has been estimated. Also, the excited energy for the nuclei are roughly calculated. There is good agreement between the noncritical holography model results and the experimental data.

DOI: 10.1103/PhysRevC.88.064004 PACS number(s): 11.25.Tq, 21.45.−v, 21.10.Dr, 27.10.+h

I. INTRODUCTION

Nuclear potential and binding energies are important issues in nuclear physics which are experimentally known with high accuracy while they are not predicted with sufficient accuracy using different theoretical models. So, the prediction of nuclear binding energy is a useful tool to test the goodness of a theoretical nucleon-nucleon (*NN*) interaction model.

There are some familiar high-quality one -boson-exchange potentials (OBEP) to describe the empirical scattering data (Nijm I, Nijm II, Reid93, CD-Bonn, AV18), but they contain a large number of purely phenomenological parameters [1–5]. Also, there are many attempts to impose the symmetries of QCD using an effective Lagrangian of pions and nucleons [6,7]. Despite many efforts, no potential model has yet been constructed which gives a high-quality description of the empirical data, obeys the symmetries of QCD, and contains only a small number of free phenomenological parameters.

One of the applications of anti–de Sitter space/conformal field theory (AdS/CFT) duality [8–10] is holographic QCD introduced recently to solve the strong-coupling QCD problems such as the chiral dynamics of hadrons in particular baryons [11–35]. There are many holographic models based on the critical string theory which describe some features of QCD well such as the *SS* model. Recently, some holographic models were introduced based on the noncritical string theory as well. One of the them is composed of $D4$ and anti-$D4$ brane in six-dimensional noncritical string theory [36–38]. The low energy effective theory on the intersecting brane configuration is a four-dimensional QCD-like effective theory with the global chiral symmetry, $U(N_f)_L \times U(N_f)_R$. In this brane configuration, the six-dimensional gravity background is the near horizon geometry of the color $D4$ brane. This model is based on the compactified AdS_6 space-time with a constant dilaton. Some of the QCD features are studied in this model such as the meson spectrum [38] and the structure of the thermal phase [39]. We have studied the baryon-baryon interaction in this model [12] and obtained a realistic *NN* potential in terms of the meson exchange potential. Also, the nucleon-meson coupling constants are calculated using the AdS_6 background [12].

We believe that the noncritical holography model is more reliable than the critical model to study the *NN* interactions for some reasons. At first, the size of the baryon is of order one so our model does not suffer from the zero size of the baryon in the critical holographic model. Also, the critical holographic models have some extra *KK* modes which do not belong to the spectrum of pure *YM* theory. These undesired *KK* modes come from the extra internal space over which ten-dimensional string theory is compactified. In the noncritical holography model, which we studied here, there is no additional compactified sphere so there are no such extra *KK* modes and the QCD spectrum is clear from these unwanted *KK* modes. Thus we expect that the results of the noncritical holographic model are more reliable than the critical one.

In this paper we aim to calculate the potential of light nuclei to study binding energies of the ground state and some excited states and test our *NN* potential model presented in Ref. [12]. We construct a nuclear holographic model the same as in our previous papers [13,14] in the noncritical base and calculate the nucleus potentials as the sum of their *NN* interactions. The minimum of the ground state potential is considered as the binding energy. Also, the difference between this energy and the minimum of the excited state potential presents the excited energy for each state. In order to compute the potentials, we use the values of a nucleon-meson coupling constant which we calculate using the noncritical holography model. This paper is organized as follows. In Sec. II we briefly review the noncritical holography model and present the effective *NN* potential in terms of the meson exchange interactions. In Sec. III we construct a simple model to study light nuclei such as ^{2}D, ^{3}T, ^{3}He, and ^{4}He to obtain their potential of ground and excited states and respective binding energies. Section IV is devoted to compare the results obtained using this model with the experimental data and also the *SS* model results [13,14].

II. *NN* POTENTIAL IN THE NONCRITICAL HOLOGRAPHIC QCD MODEL

In this section, we briefly describe the noncritical AdS_6 model and review the *NN* interaction potential as presented

*m.pahlavani@umz.ac.ir
†r.morad@umz.ac.ir

in our recent paper [12]. At the end of this section, we will review the results of some meson-nucleon coupling constants which are computed using this model. In the presented noncritical model, the gravity background is generated by near-extremal $D4$ branes wrapped over a circle with the antiperiodic boundary conditions. Two stacks of flavor branes, $D4$ branes and anti-$D4$ branes, are added to this geometry as flavor probe branes. The color branes extend along the directions t, x_1, x_2, x_3, τ while the probe flavor branes fill the whole Minkowski space and stretch along the radius U extended to infinity. The strings attached color $D4$ brane to a flavor brane transform as quarks, while strings hanging between a color $D4$ and a flavor $\overline{D4}$ transform as antiquarks. The chiral symmetry breaking is achieved by a reconnection of the brane-antibrane pairs. Under the quenched approximation ($N_c \gg N_f$), the back-reactions of flavor branes with the color branes can be neglected. Just like the SS model, the τ coordinate is wrapped on a circle and the antiperiodic condition is considered for the fermions on the thermal circle. The final low energy effective theory on the background is a four-dimensional QCD-like effective theory with the global chiral symmetry $U(N_f)_L \times U(N_f)_R$ [36–38].

The near horizon gravity background is defined as [38]

$$ds^2 = \left(\frac{U}{R}\right)^2 (-dt^2 + dx_i dx_i + f(U)d\tau^2) + \left(\frac{R}{U}\right)^2 \frac{dU^2}{f(U)}, \tag{1}$$

where $f(U)$ and RR six-form field strength, $F_{(6)}$ are defined by the following relations:

$$F_{(6)} = Q_c \left(\frac{U}{R}\right)^4 dt \wedge dx_1 \wedge dx_2 \wedge dx_3 \wedge du \wedge d\tau, \qquad f(U) = 1 - \left(\frac{U_{KK}}{U}\right)^5. \tag{2}$$

The values of dilaton and $R_{\rm AdS}$ under the quenched approximation are as follows:

$$R^2_{\rm AdS} = \frac{15}{2}, \quad e^{\phi} = \frac{2\sqrt{2}}{\sqrt{3}Q_c}, \tag{3}$$

where Q_c is proportional to the number of color branes N_c.

To avoid the singularity, the coordinate τ satisfies the following periodic condition:

$$\tau \sim \tau + \delta\tau, \quad \delta\tau = \frac{4\pi R^2}{5U_{KK}}. \tag{4}$$

Also, the Kaluza-Klein mass scale of this compact dimension is

$$M_{KK} = \frac{2\pi}{\delta\tau} = \frac{5}{2}\frac{U_{KK}}{R^2}, \tag{5}$$

and dual gauge field theory for this background is non-supersymmetric.

Here there is no compact sphere like the critical holographic models, so we introduce an unwrapped $D0$ brane as a baryon vertex. There is a Chern-Simons term on the vertex world-volume which induced N_c units of electric charge on the unwrapped $D0$ brane. In accordance with the Gauss constraint, the net charge should be zero. So, one needs to attach N_c fundamental strings to the $D0$ brane. In turn, the other side of the strings should end up on the probe $D4$ branes. The baryon vertex looks like an object with N_c electric charge respect to the gauge field on the $D4$ brane whose charge is the baryon number. This $D0$ brane dissolves into the $D4$ brane and becomes an instanton soliton.

The DBI action in the Yang-Mills approximation for the $D4$ brane is written as

$$S^{D4}_{YM} = -\frac{1}{4}\mu_4(2\pi\alpha')^2 \int d^4x dw e^{-\phi} \left(\frac{U(w)}{R}\right) {\rm tr} F_{mn}F^{mn} = -\int dx^4 dw \, \frac{1}{4e^2(w)} \, {\rm tr} F_{mn}F^{mn}, \tag{6}$$

where $\mu_4 = 2\pi/(2\pi ls)^5$ and $F_{MN} = \partial_M A_N - \partial_N A_M - i[A_M, A_N]$, $(M, N = 0, 1, \ldots, 5)$ is the field strength tensor, and the A_M is the $U(N_f)$ gauge field on the $D4$ brane. Also, the new coordinate w is introduced as follows:

$$dw = \frac{R^2 U^{1/2} dU}{\sqrt{U^5 - U^5_{KK}}}, \tag{7}$$

to transform the metric to a conformally flat metric [12]. So, the energy of a point-like instanton localized at $w = 0$ is obtained as [12]

$$m^{(0)}_B = \frac{\sqrt{3/2}\, 4\pi^2 \mu_4 \, (2\,\pi\,\alpha')^2 R}{5} \, N_c \, M_{KK}. \tag{8}$$

The instanton tends to collapse to a point-like object while the Coulomb repulsions among the strings prefer a finite size for the instanton. Therefore, there is a competition between the mass of the instanton and Coulomb energy of fundamental strings. For a small instanton of size ρ with the density $D(x^i, w) \sim \rho^4/(r^2 + w^2 + \rho^2)^4$, the Yang-Mills energy is approximated as

$$\sim \tfrac{1}{6} m^{(0)}_B M^2_{KK} \rho^2, \tag{9}$$

and the five-dimensional Coulomb energy is

$$\sim \frac{1}{2} \times \frac{e(0)^2 N_c^2}{10\pi^2\rho^2}. \tag{10}$$

The size of an stable instanton comes from minimizing its total energy as follows:

$$\rho^2_{\rm baryon} \simeq \frac{\sqrt{2/3}}{2\pi^2\mu_4\,(2\,\pi\,\alpha')^2} \frac{1}{M^2_{KK}}. \tag{11}$$

In the SS model (the critical version of holographic QCD model) the size of the instanton goes to zero because of the large 't Hooft coupling limit. But in noncritical string theory, the 't Hooft coupling is of order one implying the size of instanton also be of order one. However, the baryon is still smaller than the effective length of the fifth direction $\sim 1/M_{KK}$ of the dual QCD and can be assumed as a point-like object in five dimensions. Thus the baryon at leading approximation can be treated as a point-like quantum field in five dimensions. We considered an effective action for the baryon field consist of the standard Dirac kinetic, a position-dependent mass term, the

five-dimensional gauge field and couplings between nucleon and quantum field. Therefore, a complete action for the baryon reads as

$$\int d^4x dw \Big[-i\bar{\mathcal{N}}\gamma^m D_m \mathcal{N} - i m_b(w)\bar{\mathcal{N}}\mathcal{N} + g_5(w)\frac{\rho^2_{\text{baryon}}}{e^2(w)}\bar{\mathcal{N}}\gamma^{mn}F_{mn}\mathcal{N}\Big] - \int d^4x dw \frac{1}{4e^2(w)}\ \text{tr}\, F_{mn}F^{mn}, \tag{12}$$

where D_m is a covariant derivative, ρ_{baryon} is the size of the stable instanton, and $g_5(w)$ is an unknown function with a value at $w = 0$ of $2\pi^2/3$ [23]. γ^m are the standard γ matrices in the flat space and $\gamma^{mn} = 1/2[\gamma^m, \gamma^n]$.

A four-dimensional nucleon is the localized mode at $w \simeq 0$ which is the lowest eigenmode of a five-dimensional baryon along the w direction. So, the action of the five-dimensional baryon must be reduced to the four dimension. In order to do this, one should perform the *KK* mode expansion for the baryon field $\mathcal{N}(x_\mu, w)$ and the gauge field $A(x_\mu, w)$. The baryon field can be expanded as

$$\mathcal{N}_{L,R}(x^\mu, w) = N_{L,R}(x^\mu) f_{L,R}(w), \tag{13}$$

where $N_{L,R}(x^\mu)$ is the chiral component of the four-dimensional nucleon field. Also the profile functions, $f_{L,R}(w)$ satisfy the following conditions:

$$\begin{aligned} \partial_w f_L(w) + m_b(w) f_L(w) &= m_B f_R(w), \\ -\partial_w f_R(w) + m_b(w) f_R(w) &= m_B f_L(w), \end{aligned} \tag{14}$$

in the range $w \in [-w_{\text{max}}, w_{\text{max}}]$, and the eigenvalue m_B is the mass of the nucleon mode, $N(x)$. Moreover, the eigenfunctions $f_{L,R}(w)$ obey the following normalization condition:

$$\int_{-w_{\text{max}}}^{w_{\text{max}}} dw\, |f_L(w)|^2 = \int_{-w_{\text{max}}}^{w_{\text{max}}} dw\, |f_R(w)|^2 = 1. \tag{15}$$

It is shown that the $f_L(w)$ tends to shift to the positive side of w under $w \to -w$ and the opposite behavior happens for $f_R(w)$. It is important in the axial coupling of the nucleon to the pions.

Also, the gauge field has a mode expansion at $A_z = 0$ gauge as

$$A_\mu(x, w) = i\alpha_\mu(x)\psi_0(w) + i\beta_\mu(x) + \sum_n B^{(n)}_\mu(x)\psi_{(n)}(w), \tag{16}$$

where α_μ and β_μ are related to the pion field $U(x) = e^{2i\pi(x)/f_\pi}$ by the following relations:

$$\begin{aligned} \alpha_\mu(x) &\equiv \{U^{-1/2}, \partial_\mu U^{1/2}\}, \\ \beta_\mu(x) &\equiv \tfrac{1}{2}[U^{-1/2}, \partial_\mu U^{1/2}]. \end{aligned} \tag{17}$$

By inserting the mode expansion of the baryon field and gauge field into Eq. (12), the baryon action is reduced to four dimensions. After performing integration over the extra dimension, we obtained the four-dimensional *NN* Lagrangian [12] as

$$\mathcal{L}_{\text{nucleon}} = -i\bar{N}\gamma^\mu\partial_\mu N - i m_B \bar{N}N + \mathcal{L}_{\text{vector}} + \mathcal{L}_{\text{axial}}, \tag{18}$$

and

$$\begin{aligned} \mathcal{L}_{\text{vector}} &= -i\bar{N}\gamma^\mu\beta_\mu N - \sum_{k\geqslant 0} g_V^{(k)}\bar{N}\gamma^\mu B_\mu^{(2k+1)} N, \\ \mathcal{L}_{\text{axial}} &= -\frac{i g_A}{2}\bar{N}\gamma^\mu\gamma^5\alpha_\mu N - \sum_{k\geqslant 1} g_A^{(k)}\bar{N}\gamma^\mu\gamma^5 B_\mu^{(2k)} N. \end{aligned} \tag{19}$$

It should be mentioned that there are two types of coupling constants, namely the direct magnetic coupling to the 5D gauge field strength and the minimal coupling in kinetic term. In fact $g = g_{\text{min}} + g_{\text{mag}}$ for all couplings. The various minimal coupling constants $g^{(k)}_{V,\text{min}}$, $g^{(k)}_{A,\text{min}}$ as well as the pion-nucleon axial coupling $g_{A,\text{min}}$ are calculated by suitable wave-function overlap integrals as [12]

$$\begin{aligned} g^{(k)}_{V,\text{min}} &= \int_{-w_{\text{max}}}^{w_{\text{max}}} dw\ |f_L(w)|^2\, \psi_{(2k+1)}(w), \\ g^{(k)}_{A,\text{min}} &= \int_{-w_{\text{max}}}^{w_{\text{max}}} dw\ |f_L(w)|^2\, \psi_{(2k)}(w), \\ g_{A,\text{min}} &= 2\int_{-w_{\text{max}}}^{w_{\text{max}}} dw\ |f_L(w)|^2\, \psi_0(w). \end{aligned} \tag{20}$$

Also, the magnetic coupling constants are calculated using the following integrals:

$$\begin{aligned} g^{(k)}_{V,\text{mag}} &= 2\,C_{\text{mag}} \int_{-w_{\text{max}}}^{w_{\text{max}}} dw \left(\frac{g_5(w)}{g_5(0)}\right)\left(\frac{U(w)}{U_{KK}}\right) \times |f_L(w)|^2 \partial_w \psi_{(2k+1)}(w), \\ g^{(k)}_{A,\text{mag}} &= 2\,C_{\text{mag}} \int_{-w_{\text{max}}}^{w_{\text{max}}} dw \left(\frac{g_5(w)}{g_5(0)}\right)\left(\frac{U(w)}{U_{KK}}\right) \times |f_L(w)|^2 \partial_w \psi_{(2k)}(w), \\ g_{A,\text{mag}} &= 4\,C_{\text{mag}} \int_{-w_{\text{max}}}^{w_{\text{max}}} dw \left(\frac{g_5(w)}{g_5(0)}\right)\left(\frac{U(w)}{U_{KK}}\right) \times |f_L(w)|^2\, \partial_w \psi_0(w). \end{aligned} \tag{21}$$

The parameter C_{mag} is defined as [12]

$$C_{\text{mag}} = \frac{\sqrt{3/2}\ \mu_4\,(2\,\pi\,\alpha')^2}{5}\ R\ N_c\ g_5(0)\ M_{KK}\ \rho^2_{\text{baryon}}. \tag{22}$$

Also the meson field should be written in the nucleon isospin representation. for the isoscalar mesons, such as $\omega^{(k)}$ meson, only the minimal couplings contribute while the isovector mesons couple to the nucleon from both minimal and magnetic channels [12]. We calculate the minimal and magnetic couplings for the vector mesons using the noncritical holography model. Then, by using them we obtain the $\omega^{(k)}$ and $\rho^{(k)}$ meson couplings to the nucleon for $k = 10$. These couplings along with the mass of these mesons are shown in Table I. The mass of mesons obtained by solving the eigenvalue equation of meson fields [12]. Also, we calculate the couplings

TABLE I. Numerical results for the vector meson-nucleon couplings $g_V^{(k)}$, and the couplings to the lowest ten vector mesons, $g_{\omega^{(k)}}$ and $g_{\rho^{(k)}}$, using the noncritical holographic QCD model. The vector meson mass square is in the unit of M_{KK}^2.

k	$g_{V,\mathrm{mag}}^{(k)}$	$g_{V,\mathrm{min}}^{(k)}$	$g_{\omega^{(k)}}$	$g_{\rho^{(k)}}$	m_{2k+1}^2
0	−1.9889	7.7251	11.5727	2.8630	0.5516
1	−6.8384	7.3315	10.9974	0.24	3.0593
2	−7.4493	7.2420	10.863	0.1036	7.6012
3	−4.6067	7.2211	10.8317	1.3072	14.1905
4	−4.4327	7.2147	10.8222	1.3910	22.8274
5	−6.6083	7.2133	10.8200	0.3024	33.5191
6	−6.1778	7.2137	10.8206	0.5179	46.2717
7	−4.0509	7.1740	10.7611	1.5616	60.3053
8	−4.4701	7.1725	10.7589	1.3512	76.8821
9	−6.5703	7.1714	10.7572	0.3005	95.4673

of the axial mesons and then obtained the couplings of $a^{(k)}$ and $f^{(k)}$ mesons to the nucleon. The mass of these mesons and their couplings to the nucleon are shown in Table II. The square mass of mesons are in the unit of M_{KK}^2.

Various mesons and their resonances play an special role in producing the *NN* potential. The long-range part of the *NN* potential ($r > 3$ fm) is mostly due to the one pion exchange mechanism which is the strongest component among the isospin dependent components. Isospin independent scalar mesons are responsible for the attractive interaction in the intermediate range of the potential ($0.7 < r < 2$ fm). This components are mainly responsible for the nuclear binding. Also in the phenomenological interaction models, the strength of this interaction is equal to the vector meson exchange with a minus sign. In fact the radial shapes differ considerably at short distances, ranging from attractive to repulsive. Some of these potential models just involve the scalar meson exchange and another contain the vector meson exchange interaction. We consider the vector meson exchange in our analysis which produce the strong short-range repulsion. Exchanging the vector meson ρ can explain the small attractive behavior of the odd-triplet state.

TABLE II. Numerical results for the axial vector mesons-nucleon couplings $g_A^{(k)}$, and the couplings to the lowest ten axial vector mesons, $g_{a^{(k)}}$ and $g_{f^{(k)}}$, using the noncritical holographic QCD model. The axial vector meson mass square is in the unit of M_{KK}^2.

k	$g_{A,\mathrm{mag}}^{(k)}$	$g_{A,\mathrm{min}}^{(k)}$	$g_{a^{(k)}}$	$g_{f^{(k)}}$	m_{2k}^2
1	4.2648	1.1659	2.7154	1.7489	1.5389
2	5.3813	1.0718	3.2301	1.6189	5.0877
3	7.8574	0.9692	4.4133	1.4539	10.6404
4	10.3344	0.6713	5.5028	1.0069	18.2525
5	12.8068	0.4188	6.6128	0.6282	27.9160
6	15.2780	0.3020	7.7900	0.4531	39.6300
7	17.7493	0.2743	9.0118	0.4115	53.4224
8	20.0849	0.2620	10.1734	0.3930	68.3462
9	22.528	0.2359	11.3820	0.3539	85.9293
10	24.9705	0.2061	12.5885	0.3092	105.5220

Finally, we consider the following general form for the *NN* potential as:

$$V_{NN} = V_\pi + V_{\eta'} + \sum_{k=1}^{\infty} V_{\rho^{(k)}} + \sum_{k=1}^{\infty} V_{\omega^{(k)}} + \sum_{k=1}^{\infty} V_{a^{(k)}} + \sum_{k=1}^{\infty} V_{f^{(k)}}, \tag{23}$$

which contains the pseudoscalar (π, η'), vector ($\rho^{(k)}$, $\omega^{(k)}$), and axial vector ($a^{(k)}$, $f^{(k)}$) meson exchange potentials, respectively. It should be noted that despite of the phenomenological *NN* interaction model, here we compute all of the nucleon-meson couplings contribute in the above potential using the noncritical holography model. In our calculations, the leading parts of potential come from the pseudoscalar meson π, isoscalar vector meson $\omega^{(k)}$, isovector vector meson $\rho^{(k)}$, and isovector axial vector meson $a^{(k)}$ exchange interactions. So, the holographic *NN* potential is written as [13,14]

$$V_{NN}^{\mathrm{holography}} = V_C(r) + \left(V_T^\sigma(r)\vec{\sigma}_1 \cdot \vec{\sigma}_2 + V_T^S(r) S_{12}\right) \vec{\tau}_1 \cdot \vec{\tau}_2, \tag{24}$$

where $V_C(r)$, $V_T^\sigma(r)$, and $V_T^S(r)$ are obtained as functions of holographic meson exchange potentials as [13,14]

$$V_C(r) = \sum_{k=1}^{10} \frac{1}{4\pi} \left(g_{\omega^{(k)}\mathcal{N}N}\right)^2 m_{\omega^{(k)}} y_0(m_{\omega^{(k)}} r), \tag{25}$$

$$V_T^\sigma(r) = \sum_{k=1}^{10} \frac{1}{4\pi} \left(\frac{g_{\rho^{(k)}\mathcal{N}N} M_{KK}}{2m_{\mathcal{N}}}\right)^2 \frac{m_{\rho^{(k)}}^3}{3M_{KK}^2} [2y_0(m_{\rho^{(k)}} r)] + \sum_{k=1}^{10} \frac{1}{4\pi} \left(g_{a^{(k)}\mathcal{N}N}\right)^2 \frac{m_{a^{(k)}}}{3} [-2y_0(m_{a^{(k)}} r)], \tag{26}$$

and

$$V_T^S(r) = \frac{1}{4\pi} \left(\frac{g_{\pi\mathcal{N}N} M_{KK}}{2m_{\mathcal{N}}}\right)^2 \frac{1}{M_{KK}^2 r^3} + \sum_{k=1}^{10} \frac{1}{4\pi} \left(\frac{g_{\rho^{(k)}\mathcal{N}N} M_{KK}}{2m_{\mathcal{N}}}\right)^2 \frac{m_{\rho^{(k)}}^3}{3M_{KK}^2} [-y_2(m_{\rho^{(k)}} r)] + \sum_{k=1}^{10} \frac{1}{4\pi} \left(g_{a^{(k)}\mathcal{N}N}\right)^2 \frac{m_{a^{(k)}}}{3} [y_2(m_{a^{(k)}} r)], \tag{27}$$

where

$$S_{12} = 3(\vec{\sigma}_1 \cdot \hat{r})(\sigma_2 \cdot \hat{r}) - \vec{\sigma}_1 \cdot \vec{\sigma}_2, \tag{28}$$

and

$$y_0(x) = \frac{e^{-x}}{x}, \quad y_2(x) = \left(1 + \frac{3}{x} + \frac{3}{x^2}\right) \frac{e^{-x}}{x}. \tag{29}$$

The mass of pion in the holographic model is zero and its coupling constant to the nucleon in our approach is 15.7.

III. POTENTIAL OF LIGHT NUCLEI

In this section, we aim to employ the model which we introduced in Refs. [13,14] for the light nuclei and obtain their potential using the results of noncritical holographic

NN interaction model. We assume that each nucleus consist of the point-like nucleons which sit on the some simple topological structures. Then we consider a sum of the *NN* interactions as the total nucleus potential. We use the *NN* holography potential discussed in previous section, as the *NN* interactions. The values of nucleon-meson coupling constants which are presented in Tables I and II are used in the numerical calculations.

The simplest and lightest nucleus is deuteron which contains one proton and one neutron. We assume that proton and neutron are located at a distance r from each other and consider the following potential for the deuteron:

$$V_{\text{deuteron}}^{\text{holography}} = V_C + \left(V_T^\sigma \vec{\sigma}_1 \cdot \vec{\sigma}_2 + V_T^S S_{12}\right) \vec{\tau}_1 \cdot \vec{\tau}_2, \quad (30)$$

where $V_C(r)$, $V_T^\sigma(r)$, and $V_T^S(r)$ are presented in Eqs. (14)–(16), respectively. As is well known, the spin-parity of deuteron is 1^+, so the values of spin and isospin interactions can be determined using the superselection rules

$$S_{12} = 2, \quad \vec{\sigma}_1 \cdot \vec{\sigma}_2 = 1, \quad \vec{\tau}_1 \cdot \vec{\tau}_2 = -3. \quad (31)$$

The deuteron potential has been calculated numerically and shown in Fig. 1. The minimum of this potential is considered the deuteron binding energy. We use the values of $N_c = 3$ and $m_N = 920\,\text{MeV}$. Also, we choose $M_{KK} = 0.372\,\text{GeV}$ to obtain the best value for the deuteron binding energy $E_B = -2.22\,\text{MeV}$.

The next nucleus which we considered here is tritium which is composed of three nucleons, two neutrons and one proton. We propose a equilateral triangular configuration for the tritium nucleus in which the distance between each two nucleons is r. We suppose that the total potential of the nucleus is the sum of the all nucleon-nucleon interaction potentials which are parameterized in terms of a single parameter r. In fact, the radius of the nucleus can be expresses in terms of parameter r. Finally, we write the following potential for the

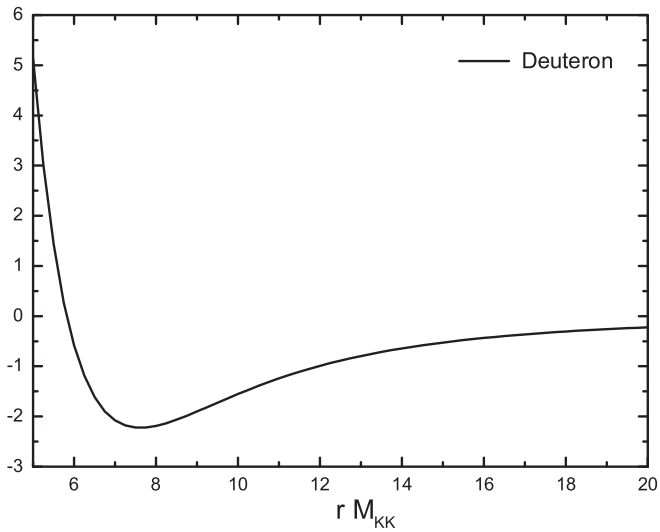

FIG. 1. The ^2D potential using the noncritical holography in MeV. The minimum of the potential is considered as the deuteron binding energy.

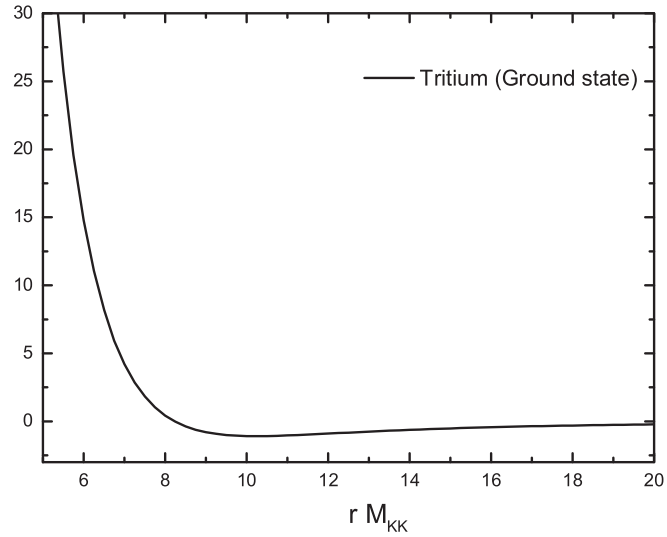

FIG. 2. The ^3T potential using the noncritical holography in MeV. The minimum of the potential is considered as the tritium binding energy.

tritium:

$$\begin{aligned} V_{\text{tritium}}^{\text{holography}} &= V_{12} + V_{13} + V_{23} \\ &= 3\,V_C(r) + \left(V_T^\sigma(r)\vec{\sigma}_1 \cdot \vec{\sigma}_2 + V_T^S(r)S_{12}\right) \vec{\tau}_1 \cdot \vec{\tau}_2 \\ &\quad + \left(V_T^\sigma(r)\vec{\sigma}_1 \cdot \vec{\sigma}_3 + V_T^S(r)S_{13}\right) \vec{\tau}_1 \cdot \vec{\tau}_3 \\ &\quad + \left(V_T^\sigma(r)\vec{\sigma}_2 \cdot \vec{\sigma}_3 + V_T^S(r)S_{23}\right) \vec{\tau}_2 \cdot \vec{\tau}_3. \end{aligned} \quad (32)$$

The superselection rules for this three-nucleon systems imply that

$$\begin{aligned} &S_{12} = 2, \quad \vec{\sigma}_1 \cdot \vec{\sigma}_2 = 1, \quad \vec{\tau}_1 \cdot \vec{\tau}_2 = -3, \\ &S_{13} = 0, \quad \vec{\sigma}_1 \cdot \vec{\sigma}_3 = -3, \quad \vec{\tau}_1 \cdot \vec{\tau}_3 = -3, \\ &S_{23} = 0, \quad \vec{\sigma}_2 \cdot \vec{\sigma}_3 = -3, \quad \vec{\tau}_2 \cdot \vec{\tau}_3 = 1. \end{aligned} \quad (33)$$

By substituting the values of $N_c = 3$, $m_N = 920$ MeV, and $M_{KK} = 600\,\text{MeV}$ in Eq. (32), the potential of tritium is calculated numerically and plotted in Fig. 2. This potential has a minimum which shows the tritium binding energy is $E_B = -8.4382\,\text{MeV}$ in this model.

In order to study the ^{3}He nucleus, it is necessary to add the repulsive Coulomb energy to the potential. So, we consider the following potential for the ^{3}He nucleus:

$$\begin{aligned} V_{^3\text{He}}^{\text{holography}} &= V_{12} + V_{13} + V_{23} \\ &= 3V_C(r) + E_c(r) \\ &\quad + \left(V_T^\sigma(r)\vec{\sigma}_1 \cdot \vec{\sigma}_2 + V_T^S(r)S_{12}\right) \vec{\tau}_1 \cdot \vec{\tau}_2 \\ &\quad + \left(V_T^\sigma(r)\vec{\sigma}_1 \cdot \vec{\sigma}_3 + V_T^S(r)S_{13}\right) \vec{\tau}_1 \cdot \vec{\tau}_3 \\ &\quad + \left(V_T^\sigma(r)\vec{\sigma}_2 \cdot \vec{\sigma}_3 + V_T^S(r)S_{23}\right) \vec{\tau}_2 \cdot \vec{\tau}_3, \end{aligned} \quad (34)$$

where $E_c(r)$ is the Coulomb repulsion between two instantons carrying N_c unit of electric charge [14]. The protons of ^{3}He in the ground state have the opposite spin directions, so the spin-parity of the ^{3}He nucleus in the ground state is $\frac{1}{2}^+$. On the other hand, we should have $L + S + T = 1$ for a system

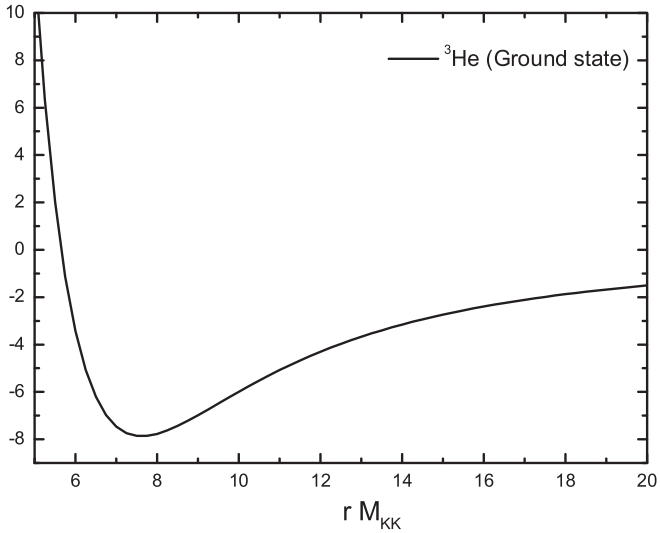

FIG. 3. The ^{3}He potential using the noncritical holography in MeV. The minimum of the potential is considered as the ^{3}He binding energy.

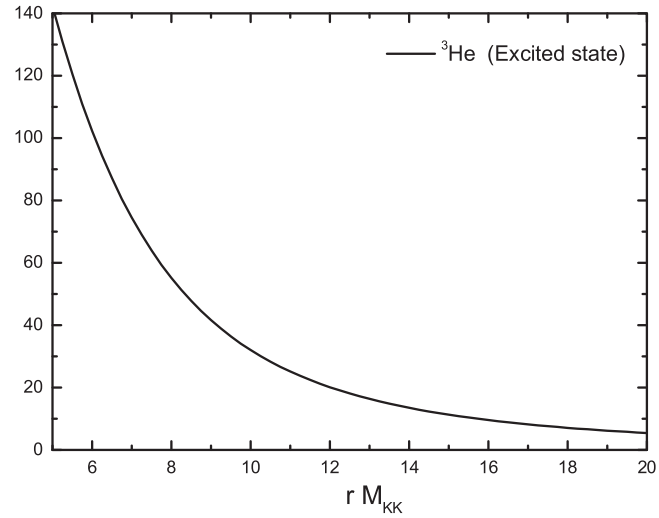

FIG. 4. The holographic potential for the excited state of the ^{3}He nucleus in MeV using the noncritical holography. As is indicated from the plot, there is no bound state in this case.

of two nucleons. It is well known that the nucleons in the ground state of the ^{3}He are in $L = 0$ state. So, by using the superselection rules we obtain

$$\begin{aligned} &S_{12} = 0, \quad \vec{\sigma}_1 \cdot \vec{\sigma}_2 = -3, \quad \vec{\tau}_1 \cdot \vec{\tau}_2 = 1, \\ &S_{13} = 2, \quad \vec{\sigma}_1 \cdot \vec{\sigma}_3 = 1, \quad \vec{\tau}_1 \cdot \vec{\tau}_3 = -3, \\ &S_{23} = 0, \quad \vec{\sigma}_2 \cdot \vec{\sigma}_3 = -3, \quad \vec{\tau}_2 \cdot \vec{\tau}_3 = 1. \end{aligned} \tag{35}$$

We choose again $M_{KK} = 372\,\text{MeV}$ and plot the total potential of this nucleus in Fig. 3. The binding energy of the ^{3}He nucleus is the minimum of this potential which is about $E_B = -7.8686\,\text{MeV}$. If we consider another sets of nucleons in ^{3}He such that the spin of protons be in a parallel direction, the spin- parity of the ^{3}He nucleus should be equal to $(\frac{3}{2})^+$. By superselection rules, we have

$$\begin{aligned} &S_{12} = 2, \quad \vec{\sigma}_1 \cdot \vec{\sigma}_2 = 1, \quad \vec{\tau}_1 \cdot \vec{\tau}_2 = 1, \\ &S_{13} = 2, \quad \vec{\sigma}_1 \cdot \vec{\sigma}_3 = 1, \quad \vec{\tau}_1 \cdot \vec{\tau}_3 = -3, \\ &S_{23} = 2, \quad \vec{\sigma}_2 \cdot \vec{\sigma}_3 = 1, \quad \vec{\tau}_2 \cdot \vec{\tau}_3 = -3. \end{aligned} \tag{36}$$

We plot the nucleus potential for this state in Fig. 4. As it is indicated from Fig. 4, there is no bound state in this case. Thus we conclude that there is no excited state for the ^{3}He nucleus, as we obtained before in the critical holography QCD model [14].

There are more than one possible configurations for a system with four nucleons. The most symmetric configurations are tetrahedron, diamond, and square configurations. If we suppose that the nucleons are located in the corners of a tetrahedron configuration which is made of four equilateral triangles, the distance between any two nucleons is similar. So, the total potential is sum of the six nucleon-nucleon interactions with a same relative distance. But, we know that the Coulomb interaction between protons prefers a larger proton-proton distance than neutron-neutron or neutron-proton distances. If two protons sit on the contrary corners of a square, then the proton-proton distance is larger than the neutron-proton distance. So, we consider the square configuration for the ^{4}He nucleus and write the potential of the ^{4}He nucleus as

$$\begin{aligned} V_{^4\text{He}}^{\text{holography}} &= V_{12} + V_{13} + V_{14} + V_{23} + V_{24} + V_{34} \\ &= 4V_C(r) + 2V_C(\sqrt{3}r) + E_c(\sqrt{2}r) \\ &\quad + \left(V_T^\sigma(r)\vec{\sigma}_1 \cdot \vec{\sigma}_2 + V_T^S(r)S_{12}\right)\vec{\tau}_1 \cdot \vec{\tau}_2 \\ &\quad + \left(V_T^\sigma(r)\vec{\sigma}_1 \cdot \vec{\sigma}_3 + V_T^S(r)S_{13}\right)\vec{\tau}_1 \cdot \vec{\tau}_3 \\ &\quad + \left(V_T^\sigma(\sqrt{2}r)\vec{\sigma}_1 \cdot \vec{\sigma}_4 + V_T^S(\sqrt{2}r)S_{14}\right)\vec{\tau}_1 \cdot \vec{\tau}_4 \\ &\quad + \left(V_T^\sigma(\sqrt{2}r)\vec{\sigma}_2 \cdot \vec{\sigma}_3 + V_T^S(\sqrt{2}r)S_{23}\right)\vec{\tau}_2 \cdot \vec{\tau}_3 \\ &\quad + \left(V_T^\sigma(r)\vec{\sigma}_2 \cdot \vec{\sigma}_4 + V_T^S(r)S_{24}\right)\vec{\tau}_2 \cdot \vec{\tau}_4 \\ &\quad + \left(V_T^\sigma(r)\vec{\sigma}_3 \cdot \vec{\sigma}_4 + V_T^S(r)S_{34}\right)\vec{\tau}_3 \cdot \vec{\tau}_4. \end{aligned} \tag{37}$$

It is well known from the Pauli exclusion rule that the spins of two protons (neutrons) have opposite directions and the ^{4}He nucleus in the ground state has the spin-parity 0^+. The superselection rules for this structure imply that

$$\begin{aligned} &S_{12} = 0, \quad \vec{\sigma}_1 \cdot \vec{\sigma}_2 = -3, \quad \vec{\tau}_1 \cdot \vec{\tau}_2 = 1, \\ &S_{13} = 2, \quad \vec{\sigma}_1 \cdot \vec{\sigma}_3 = 1, \quad \vec{\tau}_1 \cdot \vec{\tau}_3 = -3, \\ &S_{14} = 0, \quad \vec{\sigma}_1 \cdot \vec{\sigma}_4 = -3, \quad \vec{\tau}_1 \cdot \vec{\tau}_4 = 1, \\ &S_{23} = 0, \quad \vec{\sigma}_2 \cdot \vec{\sigma}_3 = -3, \quad \vec{\tau}_2 \cdot \vec{\tau}_3 = 1, \\ &S_{24} = 2, \quad \vec{\sigma}_2 \cdot \vec{\sigma}_4 = 1, \quad \vec{\tau}_2 \cdot \vec{\tau}_4 = -3, \\ &S_{34} = 0, \quad \vec{\sigma}_3 \cdot \vec{\sigma}_4 = -3, \quad \vec{\tau}_3 \cdot \vec{\tau}_4 = 1. \end{aligned} \tag{38}$$

The total potential for the ground state of the ^{4}He nucleus is plotted in Fig. 5. We choose $M_{KK} = 533\,\text{MeV}$ to obtain the ^{4}He binding energy about $E_B = -28.3527\,\text{MeV}$.

Also, the potential of ^{4}He is obtained for its excited states with $(2^-, T = 1)$, $(2^-, T = 0)$, and $(1^-, T = 1)$ by considering various structures for the spin-parity of nucleons. The holographic potential for each excited state has a minimum. The excited energies of these states can be regarded as the difference between the minimum point of a potential in each state and the binding energy of the nucleus.

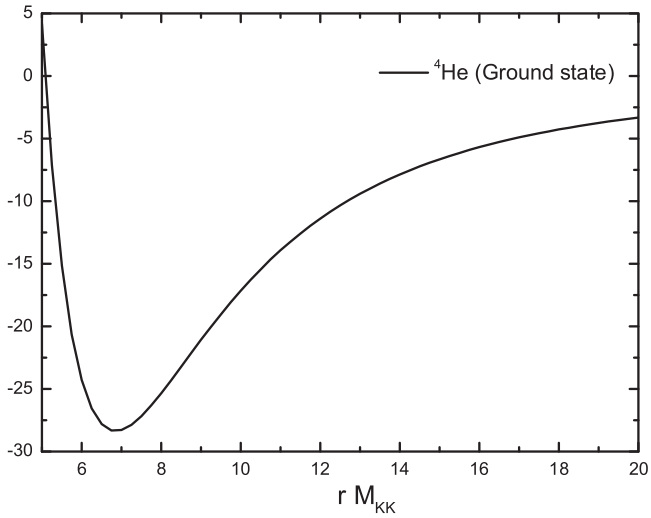

FIG. 5. The ^{4}He potential using the noncritical holography in MeV. The minimum of the potential is considered as the ^{4}He binding energy.

If two nucleons (two protons or neutron) have the same spin directions and occupy the level $L = 1$, we find the excited level with 2^-, $T = 1$ and excited energy $E_{\rm ex} = 23.330$ MeV. Superselection rules for this state lead to

$$\begin{aligned} &S_{12} = 2, \quad \vec{\sigma}_1 \cdot \vec{\sigma}_2 = 1, \quad \vec{\tau}_1 \cdot \vec{\tau}_2 = 1, \\ &S_{13} = 0, \quad \vec{\sigma}_1 \cdot \vec{\sigma}_3 = -3, \quad \vec{\tau}_1 \cdot \vec{\tau}_3 = -3, \\ &S_{14} = 2, \quad \vec{\sigma}_1 \cdot \vec{\sigma}_4 = 1, \quad \vec{\tau}_1 \cdot \vec{\tau}_4 = 1, \\ &S_{23} = 0, \quad \vec{\sigma}_2 \cdot \vec{\sigma}_3 = -3, \quad \vec{\tau}_2 \cdot \vec{\tau}_3 = 1, \\ &S_{24} = 2, \quad \vec{\sigma}_2 \cdot \vec{\sigma}_4 = 1, \quad \vec{\tau}_2 \cdot \vec{\tau}_4 = 1, \\ &S_{34} = 0, \quad \vec{\sigma}_3 \cdot \vec{\sigma}_4 = -3, \quad \vec{\tau}_3 \cdot \vec{\tau}_4 = -3. \end{aligned} \tag{39}$$

Numerical values for the potential of this excited state are shown in Fig. 6. For this state we obtain $E_{\rm ex} = 25.1005$ MeV

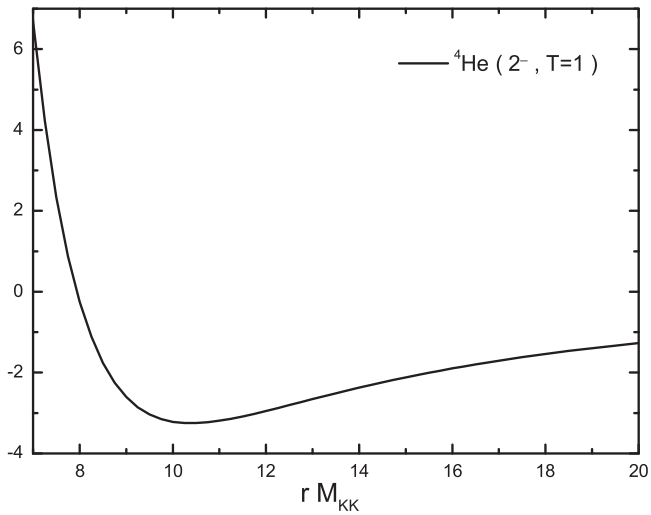

FIG. 6. The holographic potential for excited state of the ^{4}He nucleus with spin-parity 2^- and $T = 1$ in MeV using the noncritical holography.

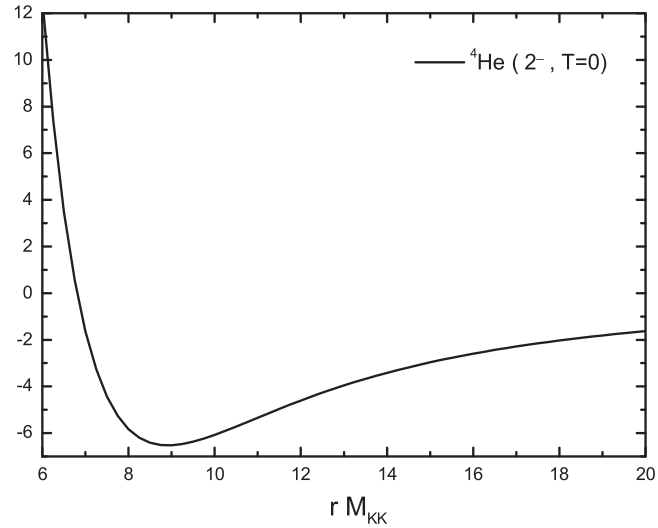

FIG. 7. The holographic potential for an excited state of the ^{4}He nucleus with spin-parity 2^- and $T = 0$ in MeV using the noncritical holography.

using the value $M_{KK} = 395$ MeV, while such excited state is not predicted by the *SS* model [14].

In another structure, we suppose that the spins of two protons (or neutrons) have the same directions and one of them occupies the $L = 1$ level. In this case, the spin-parity of the state is 2^-. It may be treated as an excited state of the ^{4}He nucleus with spin-parity and isospin 2^-, $T = 0$ and the excited energy $E_{\rm ex} = 21.840$ MeV. In order to calculate its holographic potential, the following values which are obtained from the superselection rules have been used:

$$\begin{aligned} &S_{12} = 2, \quad \vec{\sigma}_1 \cdot \vec{\sigma}_2 = 1, \quad \vec{\tau}_1 \cdot \vec{\tau}_2 = -3, \\ &S_{13} = 0, \quad \vec{\sigma}_1 \cdot \vec{\sigma}_3 = -3, \quad \vec{\tau}_1 \cdot \vec{\tau}_3 = 1, \\ &S_{14} = 2, \quad \vec{\sigma}_1 \cdot \vec{\sigma}_4 = 1, \quad \vec{\tau}_1 \cdot \vec{\tau}_4 = 1, \\ &S_{23} = 0, \quad \vec{\sigma}_2 \cdot \vec{\sigma}_3 = -3, \quad \vec{\tau}_2 \cdot \vec{\tau}_3 = 1, \\ &S_{24} = 2, \quad \vec{\sigma}_2 \cdot \vec{\sigma}_4 = 1, \quad \vec{\tau}_2 \cdot \vec{\tau}_4 = 1, \\ &S_{34} = 0, \quad \vec{\sigma}_3 \cdot \vec{\sigma}_4 = -3, \quad \vec{\tau}_3 \cdot \vec{\tau}_4 = -3. \end{aligned} \tag{40}$$

This potential has been plotted in Fig. 7. The exited energy for this state is obtained about $E_{\rm ex} = 21.8237$ MeV using the value $M_{KK} = 395$ MeV.

If the spin of proton (neutron) in the $L = 1$ level couples with the spin of the proton (neutron) in the $L = 0$ state, we find another excited state with the 1^-, $T = 1$ and the measured excited energy $E_{\rm ex} = 23.640$ MeV. In this case we have

$$\begin{aligned} &S_{12} = 2, \quad \vec{\sigma}_1 \cdot \vec{\sigma}_2 = 1, \quad \vec{\tau}_1 \cdot \vec{\tau}_2 = 1, \\ &S_{13} = 0, \quad \vec{\sigma}_1 \cdot \vec{\sigma}_3 = -3, \quad \vec{\tau}_1 \cdot \vec{\tau}_3 = -3, \\ &S_{14} = 0, \quad \vec{\sigma}_1 \cdot \vec{\sigma}_4 = -3, \quad \vec{\tau}_1 \cdot \vec{\tau}_4 = -3, \\ &S_{23} = 0, \quad \vec{\sigma}_2 \cdot \vec{\sigma}_3 = -3, \quad \vec{\tau}_2 \cdot \vec{\tau}_3 = 1, \\ &S_{24} = 0, \quad \vec{\sigma}_2 \cdot \vec{\sigma}_4 = -3, \quad \vec{\tau}_2 \cdot \vec{\tau}_4 = 1, \\ &S_{34} = 2, \quad \vec{\sigma}_3 \cdot \vec{\sigma}_4 = 1, \quad \vec{\tau}_3 \cdot \vec{\tau}_4 = -3. \end{aligned} \tag{41}$$

We substitute these values with the potential of ^{4}He nuclei and plot the potential in Fig. 8. In this case, we obtain $E_{\rm ex} = 23.658$ MeV by choosing the value $M_{KK} = 305$ MeV.

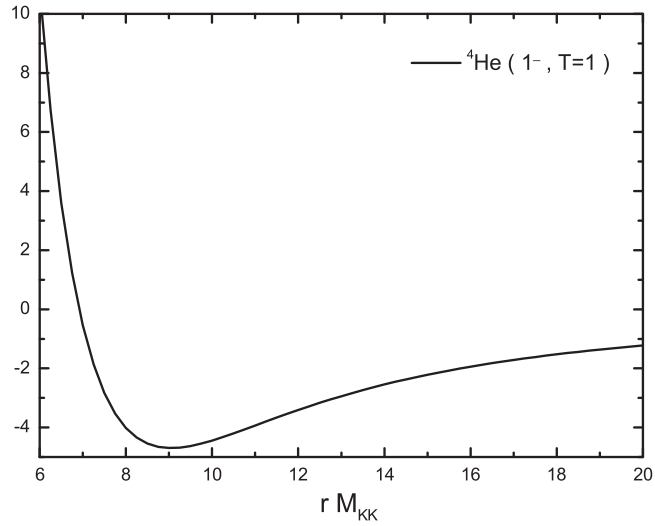

FIG. 8. The holographic potential for an excited state of the ^{4}He nucleus with spin-parity 1^- and $T = 1$ in MeV using the noncritical holography.

IV. CONCLUSION

In this paper we used the noncritical holographic version of the *NN* potential to calculate the potential of some light nuclei. The noncritical holographic *NN* potential involves only the exchanges of pions, isospin singlet mesons, isospin triplet mesons, and triplet axial-vector mesons. All nucleon-meson coupling constants employed to calculate the potentials are calculated using the noncritical AdS_6 background. We employed a toy model to calculate the nucleus potential in which the nucleons sit down in the corners of some simple geometrical structures and interact with each other by exchanging the mesons. The sum of the *NN* interactions is considered as the total nucleus potential. The number of possible configurations for a system composed of four nucleons is more than one, such as tetrahedron, square, and diamond configurations. Our potential depends on the relative distance between the nucleons of the nucleus, but we can fit the minimum of the nucleus potential by choosing the appropriate value of M_{KK}. So, we considered the diamond configuration for the ^{4}He nucleus which is more sensible because the proton-proton distance is larger than the proton-neutron and neutron-neutron distances. It is necessary to mention that our model considers a simple configuration for the nucleus in which nucleons are located at average distances. Also, by assuming the different structures for the spin and isospin of nucleons, we have calculated the potential of excited states and estimated the excited energy of nuclei.

Also, we can expand our model to study nuclei heavier than the helium nucleus. But we have to be concerned that the large number of instantonic baryons in the geometry back-reacts and deforms the geometry. In this case, we have to solve the equations of motion for the gravitating dyonic multi-instantons and find a supergravity solution. So, the toy model which we introduced can be used just for the study of light nuclei.

In general, the considered potential in this model tends to zero at $r \to \infty$ and becomes infinity at small distances which is well established for nuclear knowledge. The minimum of the potential in the ground state is considered as the binding energy of the nucleus. Moreover, the difference between the minimum of the excited state potential and the nucleus binding energy have been considered as the excited energy of the corresponding state. We applied our method for the deuteron ^{2}D, tritium ^{3}T, and two isotopes of helium, namely ^{3}He and ^{4}He nuclei.

To obtain the numerical results, $N_c = 3$ has been chosen for the realistic QCD. Also, we obtained the value of the nucleon mass at about $m_N = 0.92$ GeV which is very close to the experimental nucleon mass. In our numerical calculations there is only one free parameter M_{KK}. The results of the binding energy and excited energies are compared with results of the *SS* model and experiments in Tables III and IV. As is indicated from the tables, our results are in a good agreement with the experimental nuclear data. Moreover, our potential has only one free parameter which allows us to fit our results with the experimental data.

In Table V, we compare our numerical results for the light nuclei binding energies with the predictions of the modern

TABLE III. The obtained binding energy of ^{2}D, ^{3}T, ^{3}He, and ^{4}He nuclei with $N_c = 3$ and $m_N = 0.92$ GeV. The results have a good consistency with the experimental nuclear data [40,41]. All energies are in MeV.

Nuclei	M_{KK}	E_B^{nc}	E_B^c [13,14]	E_{exp} [40–43]
^{2}D	372	2.22	2.20	2.17 ± 0.0
^{3}T	600	8.432	1.03	8.48
^{3}He	372	7.8680	7.41	7.71
^{4}He	533	28.3527	28.58	28.30

TABLE IV. The obtained excited energy of ^{3}He and ^{4}He nuclei with $N_c = 3$ and $m_N = 0.92$ GeV. The results have a good agreement with the experimental nuclear data [40,41]. All energies are in MeV.

Nuclei	J^P	M_{KK}	E_{Ex}^{nc}	E_{Ex}^c [13,14]	$E_{\text{ex}}^{\text{exp}}$ [40,41]
^{3}He	$\frac{3}{2}^+$	–	–	–	no state
^{4}He	2^-, $T = 0$	395	21.8237	22.00	21.840
^{4}He	2^-, $T = 1$	395	25.1001	–	23.330
^{4}He	1^-, $T = 1$	305	23.658	23.17	23.640

TABLE V. $3N$ and $4N$ binding energies for various *NN* potentials [44] compared with the our holographic model results and experimental values. C-H and NC-H refer to the critical holographic [20] and noncritical holographic potential [12] models, respectively. All energies are in MeV.

Potential	$E_B(T)$	$E_B(^3\text{He})$	$E_B(^4\text{He})$
CD Bonn	−8.012	−7.272	−26.26
AV18	−7.623	−6.924	−24.28
Nijm I	−7.736	−7.085	−24.98
Nijm II	−7.654	−7.012	−24.56
C-H	−1.03	−7.41	−28.58
NC-H	−8.4320	−7.8680	−28.3527
Exp	−8.48	−7.72	−28.30

TABLE VI. Comparison of the ^{4}He binding energy obtained from our model with the results of some other theoretical models based on chiral low-momentum interactions [45,46].

Method	$E_B(^4\text{He})$ [MeV]
Faddeev-Yakubovsky	−28.65(5)
Hyperspherical harmonics	−28.65(2)
CCSD (CC with singles and doubles)	−28.44
Λ-CCSD(T) (CC with triples corrections)	−28.63
Critical holography model (*SS* model)	−28.58
Noncritical holography model(AdS_6 model)	−28.3527

phenomenological *NN* potential models [44]. It is obvious that our results obtained using the noncritical holographic *NN* potential have a significant agreement with the experimental data. It should be noted that we calculated all of the parameters of the noncritical holographic *NN* potential [12] and also, our toy model for calculating the binding energy has just one free parameter which is the mass scale of the model, M_{KK}.

Also, we compare our results for the ^{4}He binding energy with the results obtained from other methods [45,46], such as Faddeev-Yakubovsky, hyperspherical harmonics, CCSD (CC with singles and doubles), and Λ-CCSD(T) (CC with triples corrections) in Table VI. It is necessary to mention that our model depends on just one parameter which is M_{KK}, whereas the other theoretical models in nuclear literature have more than one parameter.

[1] V. Stoks and J. J. de Swart, Phys. Rev. C **47**, 761 (1993).
[2] V. G. J. Stoks, R. A. M. Klomp, C. P. F. Terheggen, and J. J. deSwart, Phys. Rev. C **49**, 2950 (1994).
[3] R. Machleidt, Phys. Rev. C **63**, 024001 (2001).
[4] R. B. Wiringa, V. G. J. Stoks, and R. Schiavilla, Phys. Rev. C **51**, 38 (1995).
[5] V. G. J. Stoks, R. A. M. Klomp, M. C. M. Rentmeester, and J. J. de Swart, Phys. Rev. C **48**, 792 (1993).
[6] C. Ordonez, L. Ray, and U. van Kolck, Phys. Rev. C **53**, 2086 (1996).
[7] Th. A. Rijken and V. G. J. Stoks, Phys. Rev. C **54**, 2851 (1996).
[8] J. Maldacena, Int. J. Theor. Phys. **38**, 1113 (1999).
[9] E. Witten, Adv. Theor. Math. Phys. **2**, 253 (1998).
[10] J. L. Petersen, Int. J. Mod. Phys. A **14**, 3597 (1999).
[11] E. Witten, J. High Energy Phys. 07 (1998) 006.
[12] M. R. Pahlavani, J. Sadeghi, and R. Morad, Phys. Rev. C **87**, 065202 (2013).
[13] M. R. Pahlavani, J. Sadeghi, and R. Morad, Phys. Rev. C **82**, 025201 (2010).
[14] M. R. Pahlavani, J. Sadeghi, and R. Morad, J. Phys. G: Nucl. Part. Phys. **38**, 055002 (2011).
[15] M. R. Pahlavani, J. Sadeghi, and R. Morad, J. Phys. G: Nucl. Part. Phys. **39**, 065004 (2012).
[16] J. Sadeghi, M. R. Pahlavani, R. Morad, and S. Heshmatian, Int. J. Theor. Phys. **50**, 488 (2011).
[17] K. Nawa, H. Suganuma, and T. Kojo, Phys. Rev. D **75**, 086003 (2007).
[18] D. K. Hong, T. Inami, and H. U. Yee, Phys. Lett. B **646**, 165 (2007).
[19] D. K. Hong, M. Rho, H. U. Yee, and P. Yi, Phys. Rev. D **76**, 061901 (2007).
[20] D. K. Hong, M. Rho, H. U. Yee, and P. Yi, J. High Energy Phys. 09 (2007) 063.
[21] Y. Kim, S. Lee, and P. Yi, J. High Energy Phys. 04 (2009) 086.
[22] H. Hata, T. Sakai, S. Sugimoto, and S. Yamato, Prog. Theor. Phys. **117**, 1157 (2007).
[23] S. Seki and J. Sonnenschein, J. High Energy Phys. 01 (2009) 053.
[24] O. Bergman, G. Lifschytz, and M. Lippert, J. High Energy Phys. 11 (2007) 056.
[25] M. Rozali, H.-H. Shieh, M. Van Raamsdonk, and J. Wu, J. High Energy Phys. 01 (2008) 053.
[26] H. Hata and M. Murata, Prog. Theor. Phys. **119**, 461 (2008).
[27] H. Hata, M. Murata, and S. Yamato, Phys. Rev. D **78**, 086006 (2008).
[28] K.-Y. Kim, S.-J. Sin, and I. Zahed, J. High Energy Phys. 07 (2008) 096.
[29] J. Park and P. Yi, J. High Energy Phys. 06 (2008) 011.
[30] O. Bergman, G. Lifschytz, and M. Lippert, Phys. Rev. D **79**, 105024 (2009).
[31] K.-Y. Kim and I. Zahed, J. High Energy Phys. 09 (2008) 007.
[32] K. Hashimoto, Prog. Theor. Phys. **121**, 241 (2009).
[33] A. Pomarol and A. Wulzer, Nucl. Phys. B **809**, 347 (2009).
[34] K. Nawa, H. Suganuma, and T. Kojo, Phys. Rev. D **79**, 026005 (2009).
[35] A. Dymarskya, D. Melnikovb, and J. Sonnenschein, J. High Energy Phys. 06 (2011) 145.
[36] S. Kuperstein and J. Sonnenschein, J. High Energy Phys. 07 (2004) 049.
[37] F. Bigazzi, R. Casero, A. L. Cotrone, E. Kiritsis, and A. Paredes, J. High Energy Phys. 10 (2005) 012.
[38] R. Casero, A. Paredes, and J. Sonnenschein, J. High Energy Phys. 01 (2006) 127.
[39] V. Mazu and J. Sonnenschein, J. High Energy Phys. 06 (2008) 091.
[40] G. Audia, O. Bersillonb, J. Blachotb, and A. H. Wapstra, Nucl. Phys. A **624**, 1 (1997).
[41] D. R. Tilley and H. R. Weller, Nucl. Phys. A **541**, 1 (1992).
[42] F. T. Rogers, Jr. and Marguerite M. Rogers, Phys. Rev. **55**, 263 (1939).
[43] A. Stadler and F. Gross, Phys. Rev. Lett. **78**, 26 (1997).
[44] A. Nogga, H. Kamada, and W. Gloeckle, Phys. Rev. Lett. **85**, 944 (2000).
[45] A. Nogga, Few Body Syst. **43**, 137 (2008).
[46] S. Bacca, A. Schwenk, G. Hagen, and T. Papenbrock, Eur. Phys. J. A **42**, 553 (2009).